AIP | Applied Physics Letters

High quality HfO2/p-GaSb(001) metal-oxide-semiconductor capacitors with 0.8nm equivalent oxide thickness

Michael Barth, G. Bruce Rayner Jr., Stephen McDonnell, Robert M. Wallace, Brian R. Bennett, Roman Engel-Herbert, and Suman Datta

Citation: Applied Physics Letters **105**, 222103 (2014); doi: 10.1063/1.4903068
View online: http://dx.doi.org/10.1063/1.4903068
View Table of Contents: http://scitation.aip.org/content/aip/journal/apl/105/22?ver=pdfcov
Published by the AIP Publishing

High quality HfO_2/p-GaSb(001) metal-oxide-semiconductor capacitors with 0.8 nm equivalent oxide thickness

Michael Barth,[1] G. Bruce Rayner, Jr.,[2] Stephen McDonnell,[3] Robert M. Wallace,[3] Brian R. Bennett,[4] Roman Engel-Herbert,[5,a)] and Suman Datta[1,b)]
[1]*Department of Electrical Engineering, The Pennsylvania State University, University Park, Pennsylvania 16802, USA*
[2]*Kurt J. Lesker Company, Pittsburgh, Pennsylvania 15025, USA*
[3]*Department of Materials Science and Engineering, University of Texas at Dallas, Richardson, Texas 75080, USA*
[4]*Naval Research Laboratory, Washington, DC 20357, USA*
[5]*Department of Material Science and Engineering, The Pennsylvania State University, University Park, Pennsylvania 16802, USA*

(Received 14 October 2014; accepted 18 November 2014; published online 2 December 2014)

We investigate *in-situ* cleaning of GaSb surfaces and its effect on the electrical performance of p-type GaSb metal-oxide-semiconductor capacitor (MOSCAP) using a remote hydrogen plasma. Ultrathin HfO_2 films grown by atomic layer deposition were used as a high permittivity gate dielectric. Compared to conventional *ex-situ* chemical cleaning methods, the *in-situ* GaSb surface treatment resulted in a drastic improvement in the impedance characteristics of the MOSCAPs, directly evidencing a much lower interface trap density and enhanced Fermi level movement efficiency. We demonstrate that by using a combination of *ex-situ* and *in-situ* surface cleaning steps, aggressively scaled HfO_2/p-GaSb MOSCAP structures with a low equivalent oxide thickness of 0.8 nm and efficient gate modulation of the surface potential are achieved, allowing to push the Fermi level far away from the valence band edge high up into the band gap of GaSb. © *2014 AIP Publishing LLC*. [http://dx.doi.org/10.1063/1.4903068]

Antimonide (Sb) III-V compound semiconductor, such as GaSb, exhibits remarkable hole transport properties, with low effective mass and high carrier mobility at room temperature making them attractive as p-channel material to replace silicon in metal-oxide-semiconductor field effect transistors (MOSFETs)[1] and p-type tunnel field effect transistors,[2] as well as for use in infrared optoelectronics.[3,4] However, GaSb is not stable at ambient conditions, forming a native oxide with complex chemistry on the surface. Reducing and controlling the phases present in the GaSb oxide overlayer have been identified as critical road blocks towards high performance Sb-based electronic devices, which imposes stringent process requirements for device fabrication and integration of a high quality gate oxide.[5]

The GaSb (001) surface is composed of long Sb-dimer chains.[6,7] However, unlike arsenide and other antimonide III-V compounds that form a $c(4 \times 4)$ reconstruction,[6] the Sb-rich GaSb surface is stabilized by randomly ordered subsurface Ga antisite defects in order to satisfy the electron counting rule (ECR).[6] During exposure to atmosphere, the GaSb surface readily forms a native oxide composed Ga_2O_3, Sb_2O_4, Sb_2O_3.[8–12] At temperatures above 200 °C, additional elemental Sb is formed as a result of the reaction between Sb-oxide and the underlying GaSb surface,[11] which is assumed to have an adverse effect, since the Sb rich native oxide/GaSb interface suffers from high interface state density (D_{it}) leading to Fermi level pinning.[13]

Recent first principle studies of HfO_2/GaSb interfaces formed on Ga-terminated surfaces have suggested that gap states were absent at oxygen-rich interfaces without direct Sb-O bonds. The Ga dangling bonds as well as Sb-Sb antibonding states were predicted to be located above the conduction band edge.[5] Therefore, to avoid the formation of the native oxide, past effort has focused on deposition of high-κ dielectrics directly on epitaxial GaSb in an ultra high vacuum (UHV) environment immediately following GaSb growth.[14] However, this UHV *in-situ* dielectric growth approach is very limiting and a more flexible approach to remove native oxides—is needed for device applications. Wet chemical etchants[15–18] high temperature thermal desorption,[10–12,19,20] capping layers,[21,22] and hydrogen cleaning[8–10] have all been explored as ways to remove the native oxide from GaSb. A limitation with *ex-situ* chemical surface pretreatments is that the native oxide can begin to reform following removal from the chemical clean.[9] Thermal oxide desorption (TOD)[20] and hydrogen cleaning[8,9] have been shown to remove the GaSb native oxide prior to atomic layer deposition (ALD). Previous work has shown the successful reduction of native oxides from and integration of Al_2O_3 on GaSb using H_2 plasma.[8,9] However, the dielectric constant of Al_2O_3 ($\epsilon = 9$) was too low to be compatible with future scaled field effect transistors. A gate oxide with higher dielectric constant such as HfO_2 ($\epsilon = 20$) is required. In this letter, we demonstrate the optimization and integration of a highly scaled HfO_2 gate dielectric deposited in an ALD reactor on p-GaSb using an *in-situ* remote hydrogen plasma.

A 500-nm-thick epitaxial p-type (Be-doped 2×10^{17} cm^{-3}) GaSb film was grown by molecular beam epitaxy (MBE) on unintentionally doped GaSb(001) substrates. H_2 plasma surface treatment, HfO_2 deposition, and post-deposition forming gas anneal (FGA) were performed *in-situ*

a)rue2@psu.edu
b)sdatta@engr.psu.edu

using a Kurt J. Lesker Co. ALD-150LX reactor equipped with a remote 13.56 MHz RF inductively coupled plasma (ICP) source. Prior to loading into the load-lock, the GaSb samples were degreased in acetone and isopropyl alcohol for 10 min each followed by hydrochloric acid (HCl) and water HCl:H2O(1:1) clean for 40 s to remove the native oxide.[16] After pump down and loading into the ALD reactor, a 100 W RF H_2 plasma treatment was performed at a substrate temperature of 110 °C with H_2 and Ar gas flows of 3 and 110 sccm, respectively, and a chamber pressure of 1 Torr. Following the H_2 plasma clean, the GaSb surfaces were exposed to ten 50 ms long prepulses of trimethylaluminum (TMA) followed by ten 50 ms long pulses of H_2O. The prepulsing was performed to effectively hydroxylate the GaSb surface and facilitate the subsequent nucleation and growth of HfO_2. The substrate temperature was subsequently increased to 250 °C, and a 3.5-nm-thick HfO_2 was deposited using alternate cycles of tetrakis(dimethylamino)hafnium [$Hf(NME_2)_4$] and H_2O. The HfO_2 process was calibrated on Si ($\epsilon_{HfO_2} = 20$). Following HfO_2 deposition, the samples underwent an *in-situ* FGA. The FGA was done at 350 °C with an H_2/Ar ambient (40 sccm of H_2 and 110 sccm of Ar). Gate metal contacts were deposited by thermal evaporation of Ni using a shadow mask. To study the effectiveness of the H_2 plasma cleaning, additional control samples were processed that have either undergone (a) *ex-situ* HCl only (no *in-situ* H_2 plasma clean) or (b) *in-situ* H_2 plasma clean only (i.e., no HCl pre-clean). The pre-pulsing and ALD conditions were the same for all treatments.

To image the high-k/III-V interface, high resolution transmission electron microscopy (HRTEM) was performed using an FEI Titan3 dual aberration corrected S/TEM operated at 300 kV, and equipped with a SuperX Energy Dispersive Spectrometry (SuperX EDS) system. Mechanical polishing was used to prepare a cross section of the GaSb metal-oxide-semiconductor capacitor (MOSCAP) with 3.5 nm of HfO_2 cleaned with *ex-situ* (1:1) HCl:H_2O and 1.5 min *in-situ* H_2 plasma. To further investigate the chemical nature of the interlayer, *ex-situ* X-ray photoelectron spectroscopy (XPS) was utilized to study the effect of low temperature H_2 plasma clean on the GaSb surface. For the XPS study, a monochromatic Al Kα ($h\upsilon = 1486.7$ eV) source and an Omicron EA125 hemispherical analyzer were utilized. The pass energy employed for this study was 15 eV, and the uncertainty of the binding energy was estimated to 0.05 eV. For quantitative analysis, the software AAnalyzer was used.[23]

Capacitance-voltage (CV) measurements were carried out in the dark at room temperature in the frequency range from 1 kHz to 1 MHz using an LCR meter (Agilent 4284 A). Fig. 1 shows the CV characteristics and distribution of D_{it} extracted by Terman method[24] for GaSb MOSCAPs cleaned with ((a)–(b)) conventional *ex-situ* (1:1) HCl:H_2O, ((c)–(d)) *in-situ* 1.5 min H_2 plasma, and ((e)–(f)) combined *ex-situ*

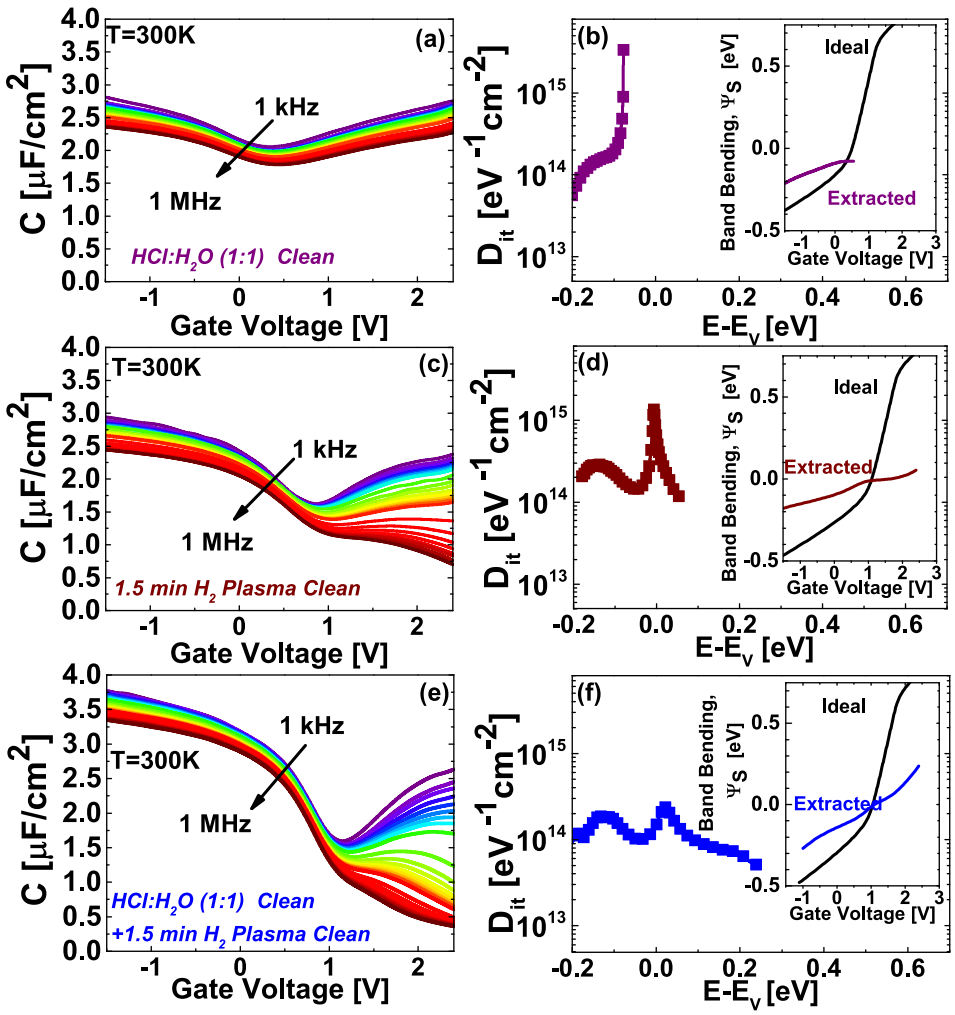

FIG. 1. CV characteristics as a function of frequency (1 kHz-1 MHz) and D_{it} distribution extracted for GaSb MOSCAPs with 3.5 nm of HfO_2 cleaned with ((a) and (b)) *ex-situ* (1:1) HCl:H_2O chemical wet etching, ((c) and (d)) *in-situ* 1.5 min H_2 plasma cleaning, and ((e) and (f)) combined *ex-situ* (1:1) HCl:H_2O and *in-situ* 1.5 min H_2 plasma. The insets in (b), (d), and (f) show surface band bending as a function of gate voltage, extracted from Terman method.[24]

(1:1) and *in-situ* cleaning. A direct comparison of the CV characteristics shows that *in-situ* H_2 plasma cleaning improves the surface potential modulation with gate bias compared to *ex-situ* cleaning. The combination of *ex-situ* cleaning and H_2 plasma cleaning is superior to either method alone, directly reflected in the reduced D_{it} and maximum band bending achieved. For *ex-situ* (1:1) HCl:H_2O clean, the CV exhibits pinning behavior, with minimal capacitance modulation with gate bias. For *in-situ* hydrogen clean, a substantial improvement in band bending and CV modulation, $C_{mod} = (C_{max}\text{-}C_{min})/C_{max} = 0.72$ at 1 MHz, is found. Where C_{max} is the maximum accumulation capacitance and C_{min} is the minimum depletion capacitance. Significant stretch out and dispersion in the depletion region is indicative of an interface that is still plagued with large D_{it}; however, band bending analysis revealed that the Fermi level was pushed above the flat band condition, resulting in a positive band bending. The D_{it} profile showed a 2× reduction in D_{it} at the valence band edge. The combination of both *ex-situ* and *in-situ* clean resulted in the best-behaved CV characteristics with an improvement in CV modulation to $C_{mod} = 0.86$, reduced stretch out, and improved band bending, as well as lower frequency dispersion in the depletion region. A C_{max} of 3.35 $\mu F/cm^2$ was found, an increase by almost 40%, which was attributed to a pronounced reduction of the low permittivity native oxide layer. Taking the quantum capacitance correction for GaSb into account, an equivalent oxide thickness (EOT) of 0.8 nm was determined from C_{max} (EOT = 1.0 nm without quantum capacitance correction). Compared to the *ex-situ* cleaning step, the resulting D_{it} profile showed a 13× reduction at the valence band edge.

While the combined *ex-situ* and *in-situ* surface cleaning have resulted in high C_{max} and C_{mod}, there was still a high density of interface trap states. Fig. 2 shows the frequency dependent CV characteristics and normalized parallel conductance maps ($G_p/\omega Aq$) for these MOSCAP at room temperature and 150 K. Here, G_p is the parallel conductance, ω is the angular frequency, and A is the area of the device. At 300 K, the CV behavior showed considerable frequency dispersion in the depletion region. Furthermore, the total capacitance did not reach the nominal minimum capacitance $C_{min} = 0.17\ \mu F/cm^2$. At T = 150 K, the 1 MHz semiconductor reached deep depletion. Also, the frequency dispersion in depletion was greatly reduced due to the expected suppression of interface trap response from trap levels located around midgap at lower temperatures. At 300 K, the conductance map showed relatively inefficient Fermi level movement, traced by the change in the frequency position of the normalized conductance maximum in response to gate bias. The trace of the conductance maximum is barely visible due to the relatively small positive band bending achieved at 300 K and the fact that shallower trap levels were not in resonance with the applied frequency. At 150 K, the conductance map revealed the trace of the parallel conductance maximum; this is attributed to a more efficient Fermi level movement and the resonant frequency shift to shallower trap levels at lower temperature.

The optimization of the H_2 plasma clean time that was varied between 1.5 to 5 min is shown in Fig. 3. The 1.5 min H_2 plasma exposure yielded the best performance for C_{max}, C_{mod}, and D_{it}. Increasing the plasma clean time to 2.5 min resulted in a 1.4× reduction of C_{max} from 3.35 $\mu F/cm^2$ to 2.40 $\mu F/cm^2$, which further reduced to $C_{max} = 1.85\ \mu F/cm^2$ for 5 min H_2 plasma clean time. TEM cross sectioning of the high-k/III-V interface for the GaSb MOSCAP with the optimized *ex-situ* plus *in-situ* clean was performed. An abrupt interface between the crystalline GaSb and amorphous dielectric was found, see Fig. 4(c). Elemental analysis across the interface using energy dispersive X-ray spectroscopy (EDX) revealed a 0.7-nm-thick interfacial layer with a high concentration of Ga, suggestive of the presence of a native oxide interlayer between GaSb and HfO_2 containing large amounts of gallium oxide phases. At a H_2 plasma clean time of 5 min, the interfacial layer was over 2.0 nm thick, see Fig. 4(b).

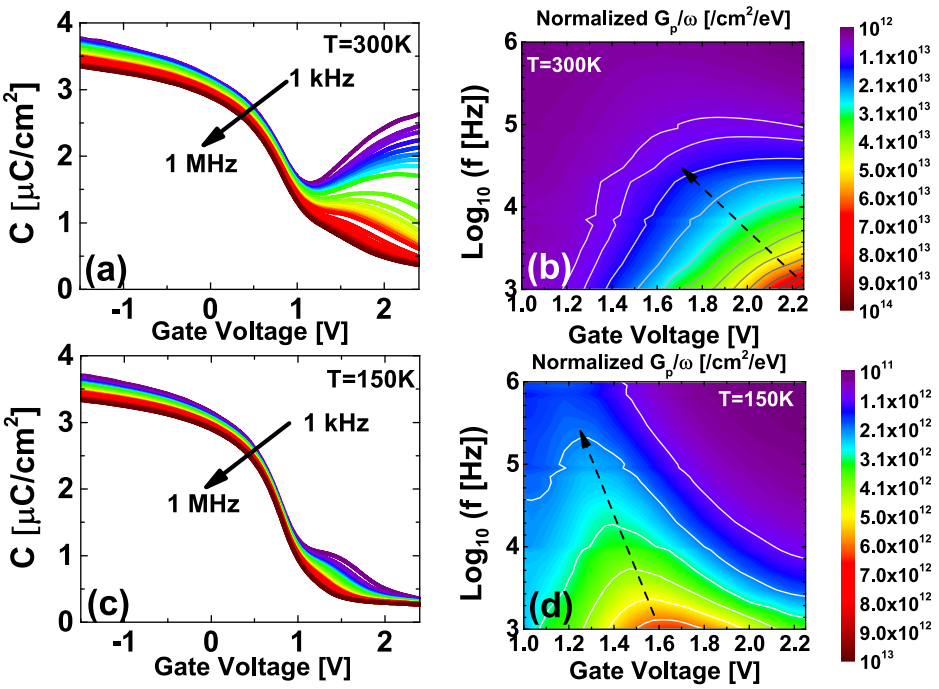

FIG. 2. Frequency dependent CV characteristics and normalized parallel conductance maps of p-type GaSb MOSCAPs with 3.5 nm HfO_2 deposited after combined surface cleaning at ((a) and (b)) T = 300 K and ((c) and (d)) T = 150 K. The dotted-line arrow in the conductance map highlights the trace of the maximum parallel conductance in the depletion region.

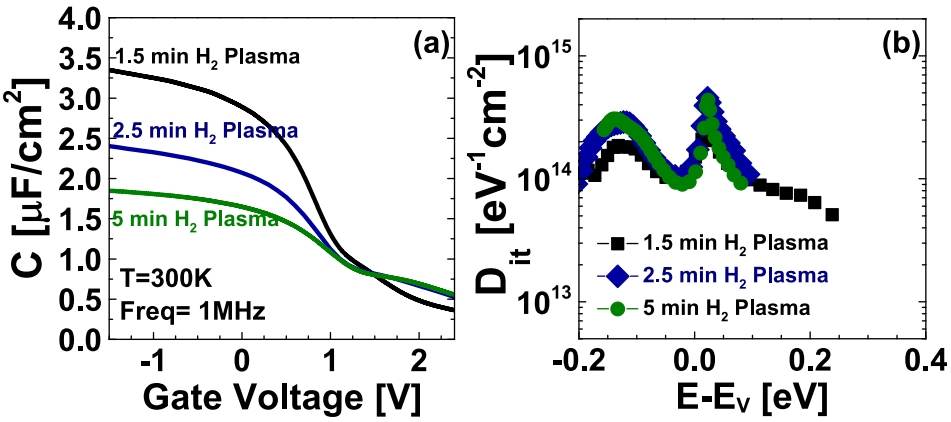

FIG. 3. (a) CV characteristics and (b) D_{it} distribution extracted from HfO_2/GaSb MOSCAPs cleaned using *ex-situ* (1:1) HCl:H_2O wet chemical etch and *in-situ* H_2 plasma with different H_2 plasma exposure times of 1.5, 2.5, and 5 min.

Fig. 5 shows the XPS high resolution spectra of the Sb 4d as well as the Ga 3d and O 2s peaks for (a) 500 nm thick GaSb epilayer with no clean treatment and GaSb surfaces treated with (b) an *ex-situ* clean, (c) an *in-situ* 1.5 min H_2 plasma clean, and (d) the combined *ex-situ* and *in-situ* cleans. To preserve the clean GaSb surface, a subsequent TMA and H_2O pre-pulse was performed at 110 °C followed by the deposition of 2 nm of Al_2O_3 deposited at 250 °C. The choice of Al_2O_3 as dielectric was to prevent the Hf peaks from interfering with the surface analysis. A relatively thick Al_2O_3 cap of 2 nm thickness was chosen to prevent significant reoxidation of the interface region due to air exposure.[25] The bare epitaxial GaSb surface showed the presence of Ga_2O_3, Sb_2O_4, and Sb_2O_3 on the GaSb surface. The assignment of Sb_2O_5 was excluded in the XPS analysis based on recent findings on the thermal decomposition of the native oxide overlayer of GaSb.[12] Sb_2O_4 is most likely the correct assigned Sb oxide phase, because it is thermodynamically preferred over Sb_2O_5 and needed to comprehensively explain the experimentally observed decomposition pathways of the GaSb native oxide overlayer.[12] All surface clean treatments showed effective removal of antimony oxide phases, with an XPS extracted Sb-O thickness of less then 0.1 nm, close to the XPS detection limit. For all treatments, the only significant Ga-oxide phase detected was Ga_2O_3. Comparison of the relative intensities of the bulk features in the Sb 4d and Ga 3d core-level spectra showed that post HCl cleaning the GaSb surface was Sb rich with a Sb/Ga ratio of 1.33. The Sb/Ga ratio for bare GaSb was 0.92, while the Sb/Ga ratio for H_2 plasma clean and HCl + H_2 plasma clean was 0.89 and 0.93, respectively.

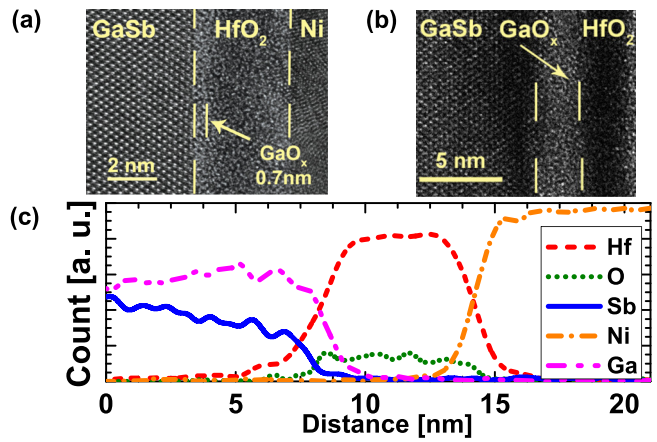

FIG. 4. (a) High resolution cross-section transmission electron micrograph of HfO_2/GaO_x/GaSb interface for *ex-situ* HCl:H_2O chemical clean followed by (a) 1.5 min and (b) 5 min H_2 plasma clean and (c) energy dispersive X-ray spectroscopy line scans taken across the HfO_2/GaSb interface for 1.5 min H_2 clean shown in (a).

We attribute the improvement in the CV characteristics with H_2 plasma clean to formation of a Ga-rich interface. For H_2 plasma cleaning, given that the initial surface likely contains Sb_2O_4 rather than Sb_2O_5 and in accordance with Weiss *et al.*,[10] we propose the following reaction pathway for the removal of the native overlayer of GaSb formed under ambient condition, containing Sb, Sb_2O_4, and Sb_2O_3:

$$2Sb_2O_4 + 16H^o \rightarrow 2Sb_2O_3 + 2H_2O \uparrow + 6H_2 \rightarrow Sb_4 \uparrow + 6H_2O. \quad (1)$$

Elemental Sb is removed via thermal desorption or through the formation of volatile SbH_3.[10] EDX revealed a lower Sb concentration relative to Ga near the GaSb/HfO_2 interface. The EDX results are consistent with the XPS results, which showed a Ga-rich GaSb interface with H_2 plasma cleaning.

At temperatures above 200 °C, GaSb can react with Sb_2O_3 to form Ga_2O_3 and elemental Sb.[11] The transfer of oxygen from Sb-O to Ga-O bond during the high temperature ALD process further enriches the interlayer with Ga oxide at these temperatures following the reaction[11]

$$2GaSb + Sb_2O_3 \rightarrow Ga_2O_3 + 4Sb. \quad (2)$$

The decomposition of Sb_2O_3 into Ga_2O_3 and Sb can explain why no Sb_2O_3 was detected post ALD process with HCl cleaning alone.

The improvement in C_{max} with the combination of *ex-situ* HCl and *in-situ* H_2 plasma cleaning over H_2 plasma alone correlates well with the XPS results. A much lower Ga-O peak intensity (layer thickness 0.6 nm) is found after the combined cleaning method compared to *in-situ* cleaning only (layer thickness 3.2 nm). The XPS extracted oxide thickness for both *ex-situ* + *in-situ* clean shows good agreement with the TEM cross-section.

The 110 °C H_2 plasma clean is unable to remove Ga_2O_3 from the GaSb surface. A minimum temperature of 250 °C (Ref. 10) is required for removal of oxide of Ga with atomic hydrogen while thermal desorption without atomic hydrogen occurred at temperatures above 500 °C.[10,11] To understand

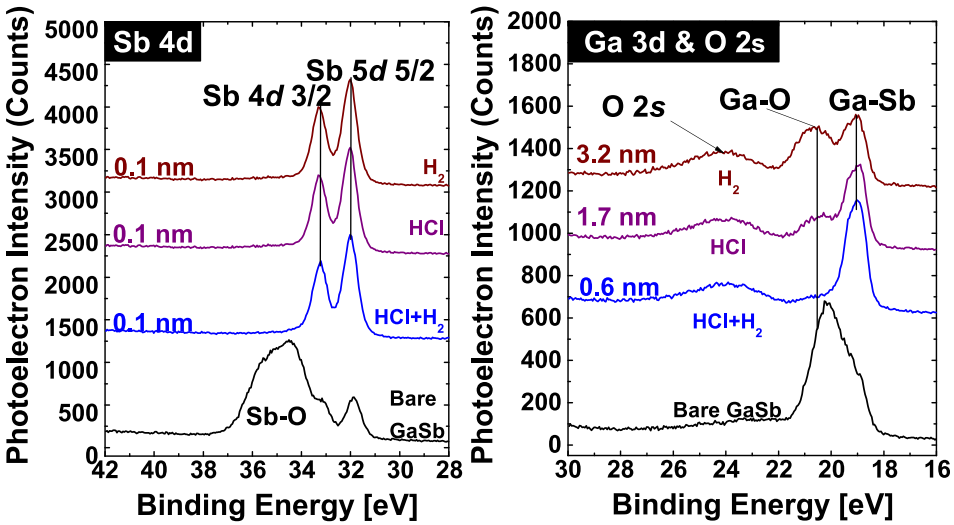

FIG. 5. High resolution X-ray photoelectron spectra of the Sb 4d as well as the O 2s & Ga 3d peaks for untreated 500 nm thick GaSb epilayer and GaSb surfaces cleaned with *ex-situ* HCl:H_2O clean, *in-situ* 1.5 min H_2 plasma clean, and combination of the *in-situ* and *ex-situ* cleaning method.

the hydrogen clean process, we consider the reaction between Ga_2O_3 and atomic hydrogen[10]

$$Ga_2O_3 + 4H^o \rightarrow Ga_2O + 2H_2O \uparrow . \quad (3)$$

It is evident from Eqs. (1) and (3) that the atomic hydrogen clean results in H_2O as a byproduct. The remaining Ga_2O [Eq. (3)] can subsequently react with this H_2O and oxidize the Ga_2O into Ga_2O_3. Additional Ga_2O_3 can also be formed due to the oxidation of Ga with these H_2O byproducts and decomposition of Ga_2O into Ga_2O_3.[9] Optimization of the H_2 plasma clean time revealed a correlation between plasma clean time and C_{max}. The TEM cross section revealed a thinner interfacial Ga_2O_3 layer with 1.5 min H_2 plasma clean compare to the 5 min clean. Lower clean time produces less interfacial Ga_2O_3, thus resulting in higher C_{max}. As the H_2 plasma clean time is increased, more elemental Sb is removed from the surface, the remaining Ga reacts with the plasma generated H_2O byproducts resulting in increased interfacial Ga_2O_3. As Ga_2O_3 is soluble in HCl solutions, the improvement in C_{max} with the *ex-situ* HCl + *in-situ* H_2 plasma clean over H_2 plasma clean alone can be ascribed to the initial removal of Ga_2O_3.

In summary, we have demonstrated the optimization of an *in-situ* H_2 plasma clean for GaSb. In combination with *ex-situ* wet chemical etch, the thickness of a Ga oxide rich low permittivity interlayer was minimized, allowing to aggressively scale HfO_2/GaSb MOSCAPs down to 0.8 nm EOT. Admittance response of the MOSCAPs showed encouraging improvements in the Fermi level movement efficiency high up into the bandgap of GaSb. Further improvements are anticipated if interlayer thickness is further reduced.

The authors thank Ke Wang from the Materials Research Laboratory at The Pennsylvania State University for his help with transmission electron microscopy. This work was supported by the Defense Threat Reduction Agency (DTRA) under Award No. HDTRA1-12-1-0026.

[1]A. Nainani, T. Irisawa, Z. Yuan, B. R. Bennett, J. B. Boos, Y. Nishi, and K. C. Saraswat, IEEE Trans. Electron Devices **58**, 3407 (2011).
[2]B. Rajamohanan, D. Mohata, D. Zhernokletov, B. Brennan, R. M. Wallace, R. Engel-Herbert, and S. Datta, Appl. Phys. Express **6**, 101201 (2013).
[3]S. A. Pour, E. K. Huang, G. Chen, A. Haddadi, B. M. Nguyen, and M. Razeghi, Appl. Phys. Lett. **98**, 143501 (2011).
[4]E. A. Plis, M. N. Kutty, and S. Krishna, Laser Photonics Rev. **7**, 45 (2013).
[5]K. Xiong, W. Wang, D. M. Zhernokletov, K. C. Santosh, R. Longo, R. M. Wallace, and K. Cho, Appl. Phys. Lett. **102**, 022901 (2013).
[6]C. Hogan, R. Magri, and R. Del Sole, Phys. Rev. Lett. **104**, 157402 (2010).
[7]L. Whitman, P. Thibado, S. Erwin, B. Bennett, and B. Shanabrook, Phys. Rev. Lett. **79**, 693 (1997).
[8]L. B. Ruppalt, E. R. Cleveland, J. G. Champlain, S. M. Prokes, J. Brad Boos, D. Park, and B. R. Bennett, Appl. Phys. Lett. **101**, 231601 (2012).
[9]E. R. Cleveland, L. B. Ruppalt, B. R. Bennett, and S. M. Prokes, Appl. Surf. Sci. **277**, 167 (2013).
[10]E. Weiss, O. Klin, S. Grossman, S. Greenberg, Klipstein, P. C., R. Akhvlediani, R. Tessler, R. Edrei, and A. Hoffman, J. Vac. Sci. Technol., A **25**, 736 (2007).
[11]G. P. Schwartz, G. J. Gualtieri, J. E. Griffiths, C. D. Thurmond, and B. Schwartz, J. Electrochem. Soc. **127**, 2488 (1980).
[12]S. McDonnell, B. Brennan, E. Bursa, R. M. Wallace, K. Winkler, and P. Baumann, J. Vac. Sci. Technol., B **32**, 041201 (2014).
[13]A. Ali, H. Madan, A. Kirk, R. Wallace, D. Zhao, A. M. H. D. A. Mourey, T. Jackson, B. Bennett, J. Boos, and S. Datta, in *Proc. 68th Annual Devices Research Conference* (IEEE, 2010), pp. 27–30.
[14]C. Merckling, X. Sun, A. Alian, G. Brammertz, V. V. Afanasev, T. Y. Hoffmann, M. Heyns, M. Caymax, and J. Dekoster, J. Appl. Phys. **109**, 073719 (2011).
[15]I. Geppert, M. Eizenberg, A. Ali, and S. Datta, Appl. Phys. Lett. **97**, 162109 (2010).
[16]Z. Y. Liu, B. Hawkins, and T. F. Kuech, J. Vac. Sci. Technol., B **21**, 71 (2003).
[17]D. M. Zhernokletov, H. Dong, B. Brennan, M. Yakimov, V. Tokranov, S. Oktyabrsky, J. Kim, and R. M. Wallace, Appl. Phys. Lett. **102**, 131602 (2013).
[18]S. McDonnell, D. M. Zhernokletov, A. P. Kirk, J. Kim, and R. M. Wallace, Appl. Surf. Sci. **257**, 8747 (2011).
[19]Z. Lu, Y. Jiang, W. Wang, M. C. Teich, and R. M. Osgood, J. Vac. Sci. Technol., B **10**, 1856 (1992).
[20]Z. Yuan, C.-Y. Chen, A. Kumar, A. Nainani, B. R. Bennett, J. B. Boos, and K. C. Saraswat, in *Proc. 71st Annual Device Research Conference* (IEEE, 2013), pp. 25–26.
[21]D. M. Zhernokletov, H. Dong, B. Brennan, J. Kim, R. M. Wallace, M. Yakimov, V. Tokranov, and S. Oktyabrsky, J. Vac. Sci. Technol., A **31**, 060602 (2013).
[22]R.-L. Chu, W.-J. Hsueh, T.-H. Chiang, W.-C. Lee, H.-Y. Lin, T.-D. Lin, G. J. Brown, J.-I. Chyi, T.-S. Huang, T.-W. Pi, J. R. Kwo, and M. Hong, Appl. Phys. Express **6**, 121201 (2013).
[23]A. Herrera-Gómez, A. Hegedus, and P. L. Meissner, Appl. Phys. Lett. **81**, 1014 (2002).
[24]R. Engel-Herbert, Y. Hwang, and S. Stemmer, Appl. Phys. Lett. **97**, 062905 (2010).
[25]S. McDonnell, H. Dong, J. M. Hawkins, B. Brennan, M. Milojevic, F. S. Aguirre-Tostado, D. M. Zhernokletov, C. L. Hinkle, J. Kim, and R. M. Wallace, Appl. Phys. Lett. **100**, 141606 (2012).